Geomechanics and Engineering, *Vol. 24, No. 1 (2021) 29-42*
DOI: https://doi.org/10.12989/gae.2021.24.1.029

A novel preloading method for foundation underpinning for the remodeling of an existing building

Chengcan Wang[1,2a], Jin-Tae Han*[2], Seokjung Kim[2b] and Young-Eun Jang[3c]

[1]*Department of Civil and Environmental Engineering, Korea University of Science and Technology, 217, Gajong-Ro, Yuseong- Gu, Daejeon-Si, Republic of Korea*
[2]*Department of Infrastructure Safety Research, Korea Institute of Civil Engineering and Building Technology, 283, Goyangdae-Ro, Ilsanseo-Gu, Goyang-Si, Republic of Korea*
[3]*Innovative SMR System Development Division, Korea Atomic Energy Research Institute, 111, Daedeok-daero, 989beon-Gil, Yuseong-Gu, Daejeon, Republic of Korea*

(Received November 12, 2020, Revised December 17, 2020, Accepted December 21, 2020)

Abstract. The utilization of buildings can be improved by extending them vertically. However, the added load of the extension might require building foundations to be underpinned; otherwise, the loads on the foundations might exceed their bearing capacity. In this study, a preloading method was presented aiming at transferring partial loads from existing piles to underpinning piles. A pneumatic-type model preloading device was developed and used to carry out centrifuge experiments to evaluate the load–displacement behavior of piles, the pile–soil interaction during preloading, and the additional loading caused by vertical extension. The results showed that the preloading devices effectively transfer load from existing piles to underpinning piles. In the additional loading test of group piles, the load-sharing ratio of a pile increased with its stiffness. The load-sharing ratio of a preloaded micropile was less than that of a non-preloaded micropile as a result of the reduction in axial stiffness caused by preloading before additional loading. Therefore, a slight reduction of the load-sharing capacity of an underpinning pile should be considered if the preloading method is applied. Further, two full scale preloading devices was developed. The devices preload underpinning piles and thereby produce reaction forces on a reaction frame to jack existing piles upward, thus transferring load from the existing piles to the underpinning piles. Specifically, screw-type and hydraulic-jack type devices were developed for the practical application of foundation underpinning during vertical extension, and their operability and load transfer effect verified via full-scale structural experiments.

Keywords: foundation underpinning; preloading device; centrifuge experiment; full-scale experiment; load-sharing ratio

1. Introduction

Owing to rapid population growth and limited space in cities, the reuse of existing buildings or existing foundations is increasing in order to decrease construction costs and periods and use land efficiently (Butcher *et al.* 2006, Laefer 2011). The South Korean government permits high-rise apartment buildings that are more than 15 years old to be remodeled and vertically extended by 2–3 floors to enhance the utilization of old existing buildings and increase housing supply (MOLIT 2013). However, the additional floors result in increased load, which existing foundations might not be able to bear. Therefore, underpinning is essential for strengthening and stabilizing the foundations of extended buildings. Numerous underpinning technologies are available to provide safe, fast, and practical support in various geotechnical situations (Essler and Yoshida 2004). Among these technologies, small-diameter grouting micropiles are commonly used because they are applicable in various ground conditions and can be installed in environments with restricted access (FHWA 2005, Bruce 1988, Qian *et al.* 2014). The extension work of high-rise apartment buildings with micropile underpinning is carried out as follows: (1) Finishing materials are removed from an existing building; (2) Holes are drilled, and underpinning micropiles are installed; (3) Additional floors are constructed, and the finishing materials are recovered.

A completed project involves complicated pile-soil-structure interactions, which comprise the interactions between existing piles (EPs) and soil, EPs and new piles, and new piles and soil. Tamura *et al.* (2012) reported the effect of EPs on new piles in terms of end and shaft resistances. The key component for the design guideline of foundation underpinning is load sharing between EPs and new piles. Several researchers have observed that the load sharing of a pile depends on its axial stiffness (Horikoshi and Randolph 1998). El Kamash and Han (2017) numerically evaluated the effect of new micropiles on underpinned foundations. Increasing micropile length reduced the vertical displacement of a foundation and increased the load carried by micropiles. Wang *et al.* (2019)

*Corresponding author, Fellow Researcher
E-mail: jimmyhan@kict.re.kr
[a]Graduate Student
E-mail: wangchengcan@kict.re.kr
[b]Senior Researcher
E-mail: seokjungkim@kict.re.kr
[c]Senior Researcher
E-mail: yejang@kaeri.re.kr

ISSN: 2005-307X (Print), 2092-6219 (Online)

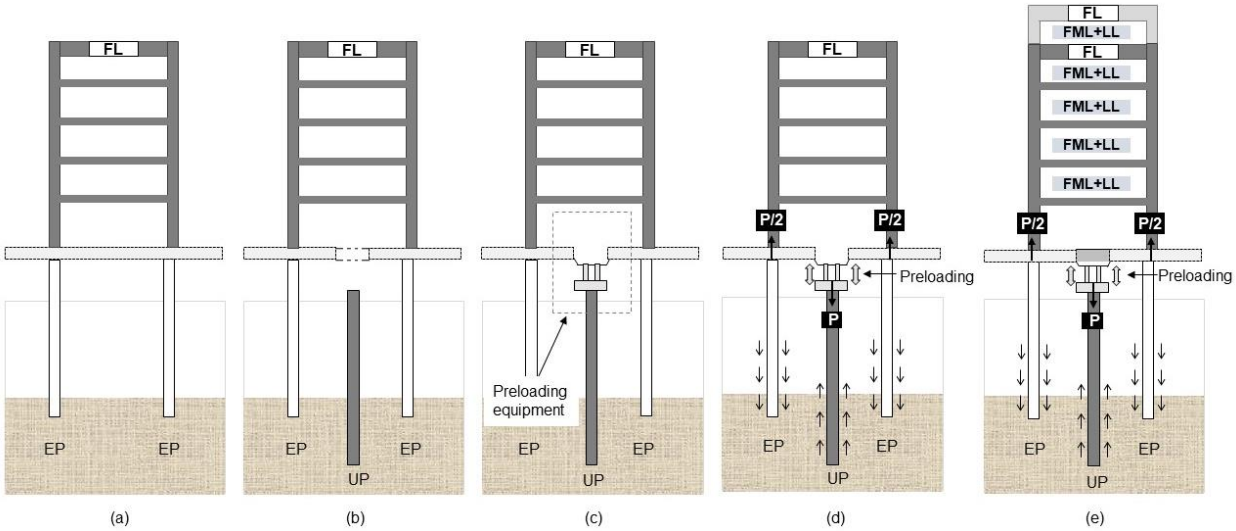

Fig. 1 Preloading in the construction of a vertical extension: (a) Existing building after removal of finishing materials, (b) drilling and installation of UP, (c) installation of preloading device, (d) application of preload and (e) vertical extension and recovery of finishing materials (FL: frame load; FML: finishing material load; LL: live load)

reported that increasing the stiffness of a micropile improved its underpinning performance in a vertically extended building.

The fundamental objective of underpinning is to share superstructural loads to ensure that the load carried by each pile does not exceed its allowable bearing capacity. Nevertheless, the allowable bearing capacity of EPs may be exceeded because the loads carried by EPs are already close to their allowable bearing capacity before vertical extension and additional loads are applied owing to vertical extension. Therefore, Wang *et al.* (2018) presented the concept of preloading UPs prior to vertical extension using a preloading device to partially reduce the loads on EPs to prevent the overloading of EPs and investigated the effectiveness of the preloading method through 3D finite element analysis. However, the constructability, applicability, and feasibility of this method at practical construction sites must be further assessed through reliable experiments to understand its mechanism. Therefore, in this paper, a model preloading device was developed for performing centrifuge tests to investigate the pile-soil interaction and load-carrying of piles during and after preloading. Moreover, this paper reports the development of two types of full-scale preloading devices for practical application. The operability of the devices was verified via full-scale structural experiments.

2. Preloading mechanism

Fig. 1 shows the preloading method applied to an underpinned foundation during vertical extension construction. The foundation includes two EPs and one UP. As shown in Fig. 1, the process involves (a) removing finishing materials from the existing building, (b) drilling a hole and placing the UP, (c) installing the preloading device on the head of the UP and fixing it to a raft; (d) applying preloading force (P in Fig. 1(d)) to the UP, and (e) building additional floors on the existing building and recovering finishing materials. The UP is pushed into the soil when preloading force P is applied to it. Uplift reaction force acts on the existing foundation against preloading force. This reduces the loads on the EPs. Subsequently, the UPs can share the load of the vertical extension. Under ideal conditions, the total decrease in the load on all EPs is equal to the increase in the load on the UP; this represents successful load transfer.

3. Verification of preloading method by centrifuge test

The full-scale structure test established the feasibility of the preloading concept and demonstrated load transfer using the devices. However, pile-soil interaction was neglected in the test. Therefore, centrifuge experiments were performed considering pile-soil interaction to evaluate 1) the load transfer mechanism during preloading, and 2) the stability of the group pile and the load sharing among piles in the subsequent loading stage of the group pile.

3.1 Preloading device for centrifuge model test

The preloading device used in the centrifuge test is shown in Fig. 2. The device consists of a pneumatic jack, a reaction frame, two air couplers, and a regulator. The reaction frame on the pneumatic jack is fixed to a raft and connected to a UP. The air couplers and regulator control the air injection velocity and injection level, respectively. The operating mechanism of this device was the same as that in the previous test. However, a different loading system was developed because turning a screw is impossible inside a spinning centrifuge. Preload was applied using the pneumatic jack, whose pneumatic pressure was controlled through a pressure channel in the centrifuge equipment even while it was spinning. When

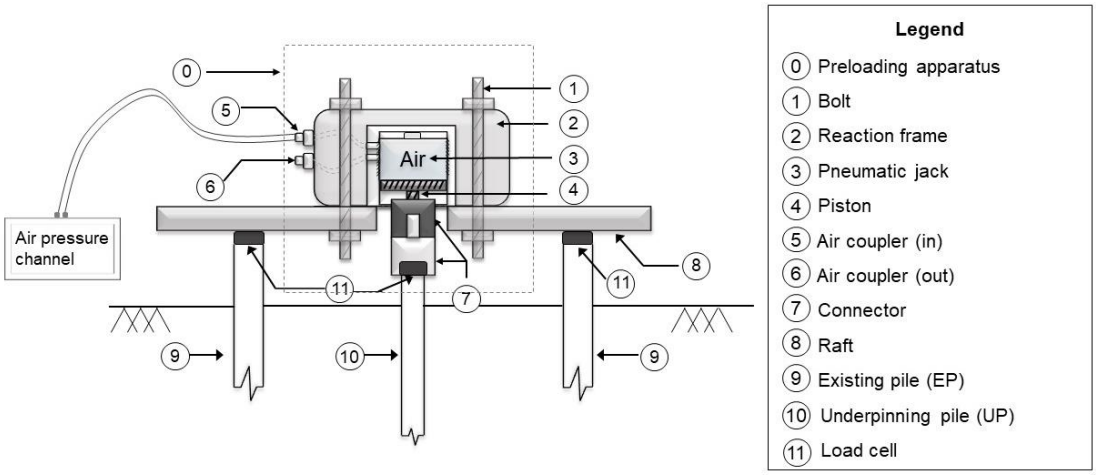

Fig. 2 Preloading device used for centrifuge test (pneumatic type)

Table 1 Specifications of the geotechnical centrifuge (Kim *et al.* 2013)

Description	Specification
Platform radius	5.0 m
Max. capacity	240 g-tons
Max. acceleration	130 g with 1,300 kg payload
Max. model payload	2,400 kg, up to 100 g
Platform dimensions	1.2 m (L) × 1.2 m (W) × 1.2 m (H)
Power consumption	220 kW for full capacity operation
Fluid rotary joint	4 lines – water and pneumatic (700 kPa) 6 lines – hydraulic oil (20 MPa)
Electrical slip rings	8 lines for electrical power supply 30 lines for signal transmission 4 channels for video transmission
Fiber-optic rotary joint	1 GHz, 2 passages

Table 2 Dimensions of model and prototype piles

Pile type		PC pile (EP)		Micropile (UP)		
		Prototype	Model	Prototype		Model
Material		Concrete	Aluminum	Grout	Steel bar	Aluminum
Young's Modulus (GPa)		40	69	37	210	69
Diameter (mm)	O.D.*	350	15	230	50	10
	I.D.*	65	13	-	-	6
Length (mm)		5635	245	10350		450
Socket length (mm)		1000	45	5700		250

*O.D. and I.D. denote the outer and inner diameters of an aluminum pipe, respectively

pneumatic pressure was applied to the preloading device, the air in the pneumatic cylinder expanded and pushed a piston. Then, the piston applied load to the UP and produced reaction forces on the reaction frame to lift the EPs upward. Thus, load was transferred from the EPs to the UP.

3.2 Experimental setup

3.2.1 Centrifuge facility

A geotechnical centrifuge is useful for the scale modeling of full-scale nonlinear geotechnical problems. Its centrifugal force increases the apparent gravitational acceleration experienced by physical models to produce identical self-weight stresses in models and prototypes. Numerous studies have used geotechnical centrifuge facilities to study the behavior of pile foundations subjected to different loading conditions (Cho *et al.* 2020, El Naggar and Sakr 2000, Horikoshi and Randolph 1996, Horikoshi *et al.* 2003, Jang and Ye 2018, Juran *et al.* 2001, Park 2018, Wang *et al.* 2016). The geotechnical centrifuge facility (maximum capacity: 240 g-tons; radius: 5 m) at the Korea Advanced Institute and Science Technology was used in this study. One of the pneumatic channels was used for air injection. Table 1 lists the specifications of the centrifuge.

3.2.2 Model piles and test cases

The prototype EPs in this test were prestressed concrete piles, which are commonly used in the deep foundations of high-rise buildings in South Korea. The micropiles were used as UPs. Table 2 presents the dimensions of the prototype and model piles obtained using appropriate scaling laws. All model piles were fabricated from aluminum (Young's modulus: 69 GPa) considering their reasonable cross-sectional dimensions. All tests were performed under a centrifugal acceleration of 23 g. Eqs. (1)-(3) provide the geometrical dimensions of the centrifuge models (Wood 2004):

$$\frac{E_p A_p}{E_m A_m} = n^2 \tag{1}$$

$$\frac{D_{EP_m}}{D_{UP_m}} = \frac{D_{EP_m}}{D_{UP_p}} \tag{2}$$

$$\frac{L_p}{L_m} = n \tag{3}$$

where D_{EPm} and D_{UPp} are the diameters of the model and prototype piles, respectively; E_p and E_m are the Young's moduli of the prototype and model piles, respectively; A_p and A_m are the cross-sectional areas of the prototype and

Table 3 Properties of silica sand

Property	Value
Specific gravity, G_s	2.65
Fraction passing #200 mesh (%)	0.9
Max. dry density, g cm^{-3}	1.63
Min. dry density, g cm^{-3}	1.28
Grain size (mm)	D_{10} = 0.19
	D_{50} = 0.32
	D_{60} = 0.34
Soil classification, USCS	SP
Uniformity coefficient, C_u	1.71
Coefficient of curvature, C_c	1.16

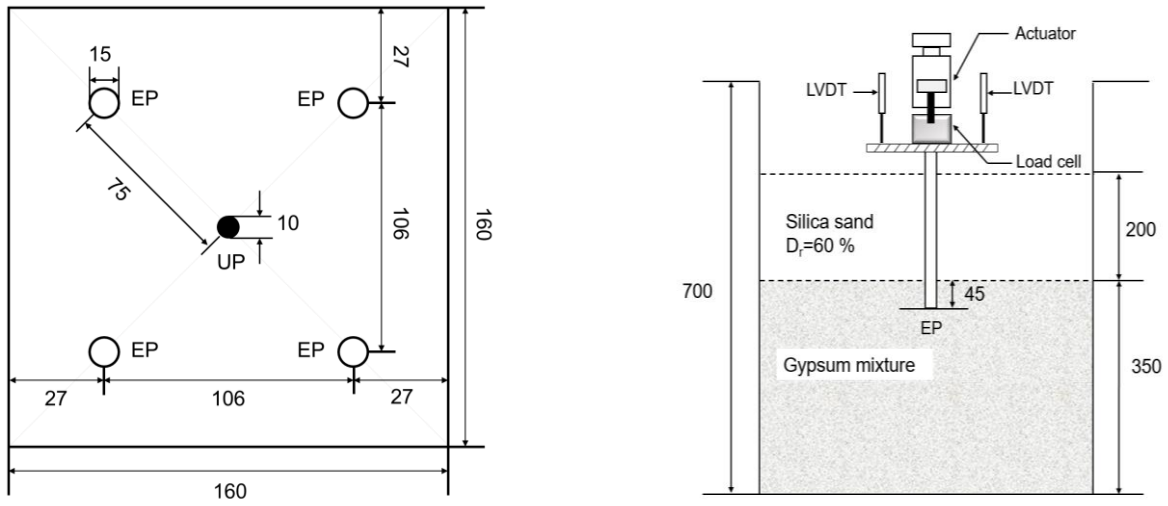

(a) Plan view of group pile

(b) Single-pile loading test (example: EP)

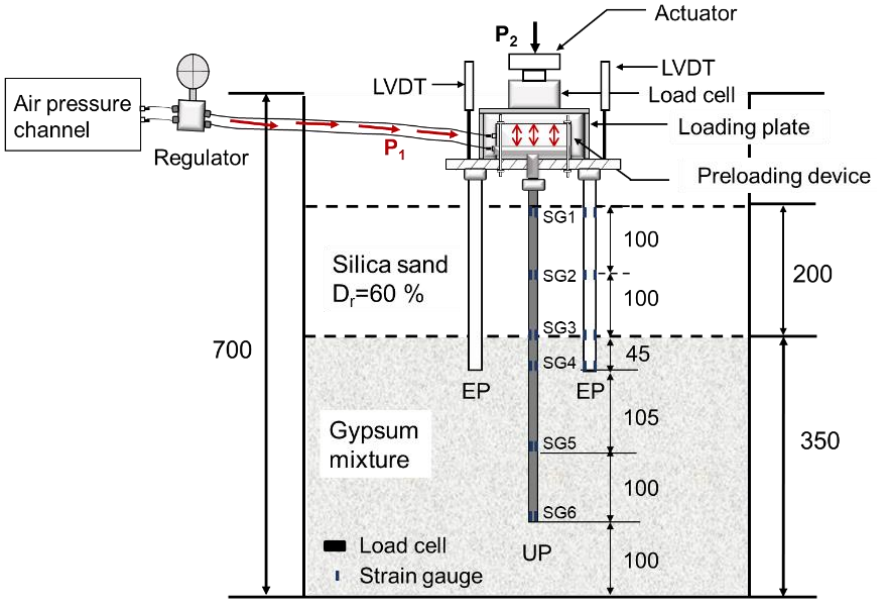

Fig. 3 Configuration and instrumentation of experimental tests (P_1: preload on the micropile; P_2: additional load on group pil after preloading; in model scale, unit: mm)

model piles, respectively; n_n is the scaling ratio, D_{UPm} and D_{EPm} are the diameters of the model and prototype piles, respectively; and L_p and L_m are the lengths of the prototype and model piles, respectively.

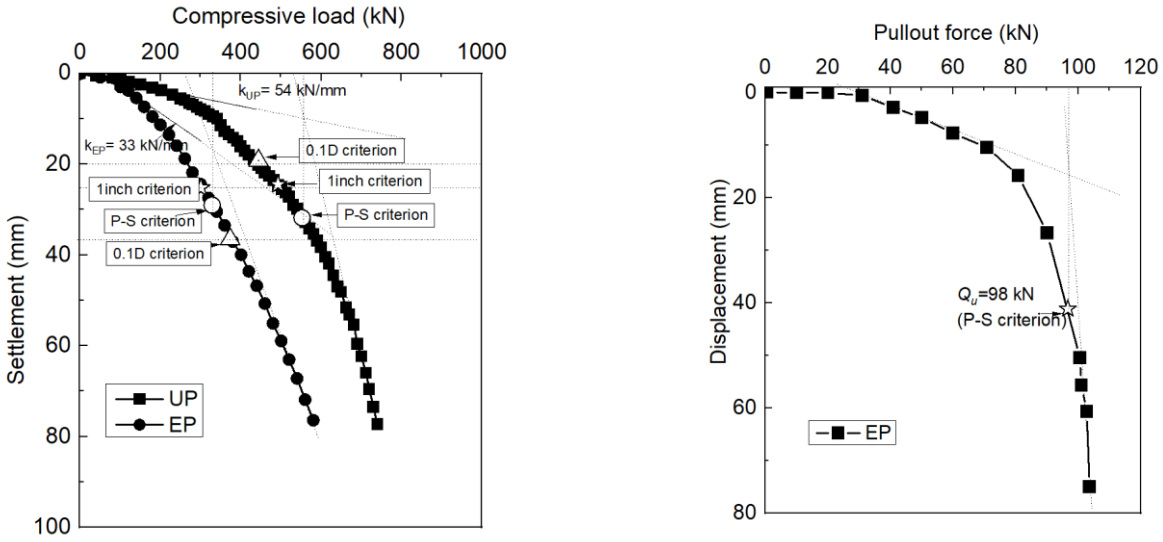

(a) Compressive loading test of piles (b) Pullout loading test of EP

Fig. 4 Load-settlement curves in single-pile loading tests (in prototype scale) (K_{EP}: stiffness of the EP; K_{UP}: stiffness of the UP; Q_{ult}: ultimate pullout capacity of the EP)

Two layers, i.e., dry silica sand and a gypsum mixture, were set to model the ground. The sand was air pluviated to prepare an upper layer with relative density D_r = 50%. Gypsum, silica sand, and water were mixed in a ratio of 1:2.3:1 and used for the bearing stratum (Leung and Ko 1993, Dykeman and Yalsangkar 1996, Seo *et al.* 2018). Owing to the complexity of the installation, model piles were set prior to the preparation of soils and the gypsum mixture was utilized to prepare a base layer in a container with a height of 350 mm. After curing for 12 days, the subsurface sand layer was prepared by air pluviating to a height of 200 mm. The detailed soil properties are listed in Table 3.

3.2.3 Model preparation

Two centrifuge model tests were carried out: single-pile loading tests and group-pile loading tests. To prevent the effect of the group pile, the spacing between each EP and the UP was set as five times the diameter of the EP, as shown in Fig. 3(a). The single-pile loading tests comprised the compressive loading tests of the EPs and UP and the pullout loading test of the EPs, which was used to evaluate the ultimate compressive bearing capacity of the piles, as shown in Fig. 3(b). The underpinned-foundation loading test used an underpinned foundation comprising four EPs and one UP. The preloading device was installed on the UP and fixed to the raft of the foundation. Two loading steps were used in this test. First, preload P_1 was applied to the UP using the preloading device. Subsequently, additional load P_2 was applied to the group-pile foundation using an actuator (Fig. 3(c)). These two steps were performed to evaluate the effect of the preloading device on the underpinned foundation and the sharing of the additional load among the piles.

Five load cells were installed on the head of each pile to measure the loads on the piles during preloading and additional loading. Four and six pairs of strain gauges were attached to both sides of one EP and one UP, respectively, to measure the axial force along the shafts of the piles during preloading. All load cells and strain gauges were calibrated at 1 g.

The single-pile and underpinned-foundation loading tests were conducted using a displacement-controlled actuator with a velocity of 0.05 mm/s. Applied loads and overall displacements were monitored using load cells and linear variable displacement transducer (LVDT) sensors, respectively. All data presented here are for the prototype scale.

4. Centrifuge test results

4.1 Single-pile loading tests

The single-pile loading tests evaluated the ultimate bearing capacity of the piles. The axial compressive load-settlement curves for the piles are shown in Fig. 4(a). The ultimate bearing capacities of the piles were estimated from these curves using existing methods; specifically, the P-S criterion, total settlement method (estimating the load corresponding to a pile head settlement of 25.4 mm), and 0.1 D method (estimating the load corresponding to a pile head settlement of 10% of the pile diameter) (Terzaghi and Peck 1967, Mayerhof 1976, British Standards 2004). The ultimate capacities obtained by these three methods were similar (Fig. 4(a)). From a relatively conservative point of view, the ultimate bearing capacities of the EP and UP were determined to be 300 kN and 500 kN, respectively, at the prototype scale by the total settlement method. The stiffness of the UP obtained by utilizing the tangent of the secant line of the load–settlement curves was 54 kN/mm, which was 1.6 times that of the EP (33 kN/mm).

Fig. 4(b) shows the plots of the pullout behavior of the EP. The tangent intersection shows that the yield pullout

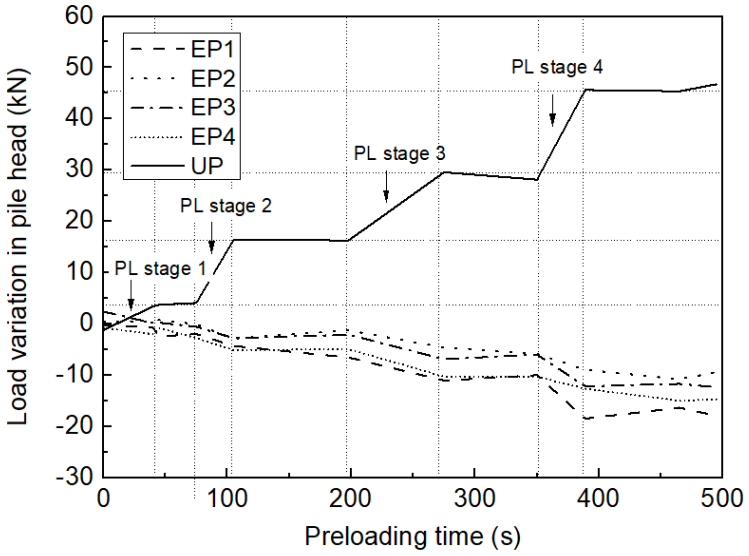

Fig. 5 Loads on piles during preloading (positive and negative values represent loading and unloading, respectively; PL: preloading)

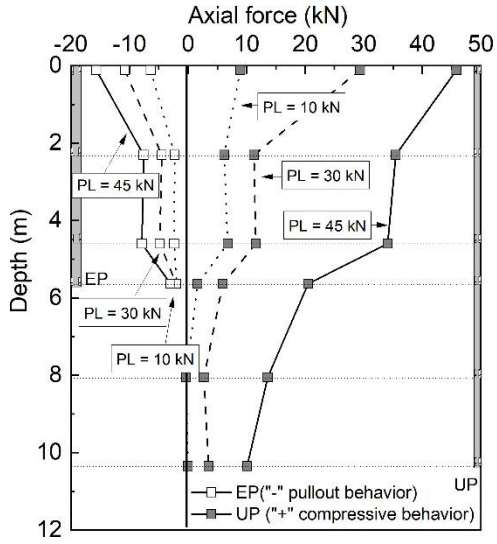

Fig. 6 Load transfer behavior of piles during preloading (PL: preloading)

capacity of the EP is 98 kN. The load-displacement response is linear until applied load reaches 50% of the ultimate load of the pile (Alawneh *et al.* 1999, Lutenegger and Gerald 1994). The pullout bearing capacity of the EP and the compressive bearing capacity of the UP were used as references for determining the preload in the subsequent preloading test.

4.2 Group-pile loading test

4.2.1 During preloading

Preloading tests were performed on the piled foundation, where pneumatic pressure was applied on the preloading device from a pneumatic channel controlled by a computer connected to the centrifuge equipment. To ensure the stability and safety of the group pile under preloading, the preload level should be within the linear elastic range of the compressive loading behavior of the UP and the pullout behavior of the EPs (Wang *et al.* 2020). Therefore, a desired preload of 45 kN (less than 10% of the ultimate capacity of the UP) controlled by a pressure regulator was applied on the UP in four preloading stages, as shown in Fig. 5.

The figure shows the variation in the loads on the piles during preloading, where positive and negative values indicate compression and tension, respectively. The loads on the EPs decrease with the preloading of the UP at each stage and remain constant when the preloading stops. These results demonstrate that the preloading of the UP results in load transfer from the EPs to the UP. This is consistent with the observations of the full-scale tests.

Fig. 6 presents the load distribution in the EPs and UP vs. depth during the preloading of the UP. Axial force was calculated by multiplying the value measured by the strain gauge with the Young's modulus and cross-sectional area of the piles provided in Table 2. The axial load on the UP increases with preload and decreases as soil depth increases. At a low preloading level, the skin friction along the upper part of the pile was mobilized. As the preloading level increased, load was gradually transferred to the pile tip. In contrast, the values of the load on the EP were negative because of the reaction force caused by preloading. This indicated that shaft resistance was mobilized in the EP so that it could resist being pulled out.

4.2.2 Additional loading on the underpinned foundation

Once the preloading of the UP was completed, additional loading tests were performed on the group pile to evaluate the load sharing among EPs and UPs. As a reference for comparison, a loading test was carried out on the underpinned foundation without preloading. Fig. 7 shows the load-settlement curves for the group pile with and without preloading. The curves show almost identical

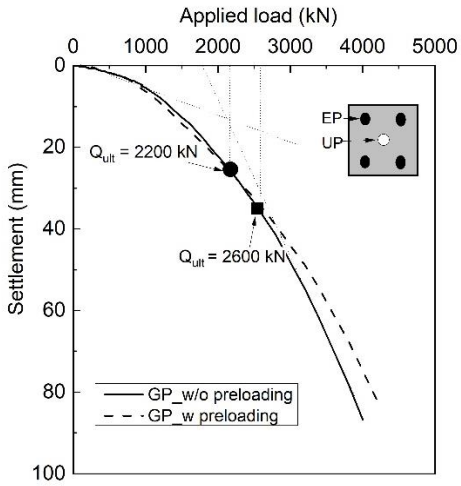

Fig. 7 Comparison of load-settlement behavior of underpinned foundation with and without preloading (Q_{ult}: ultimate capacity of the foundation)

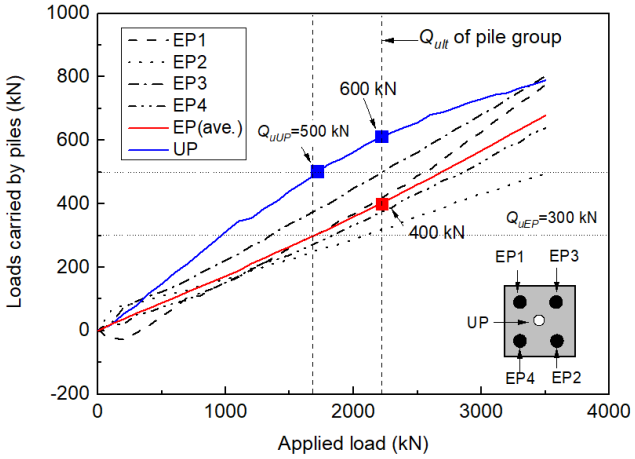

Fig. 8 Load-sharing behavior of the EPs and UP under additional loading on the raft without preloading ($Q_{ult:}$ 2200 kN, is the ultimate bearing capacity of the underpinned foundation without preloading obtained in Fig. 13)

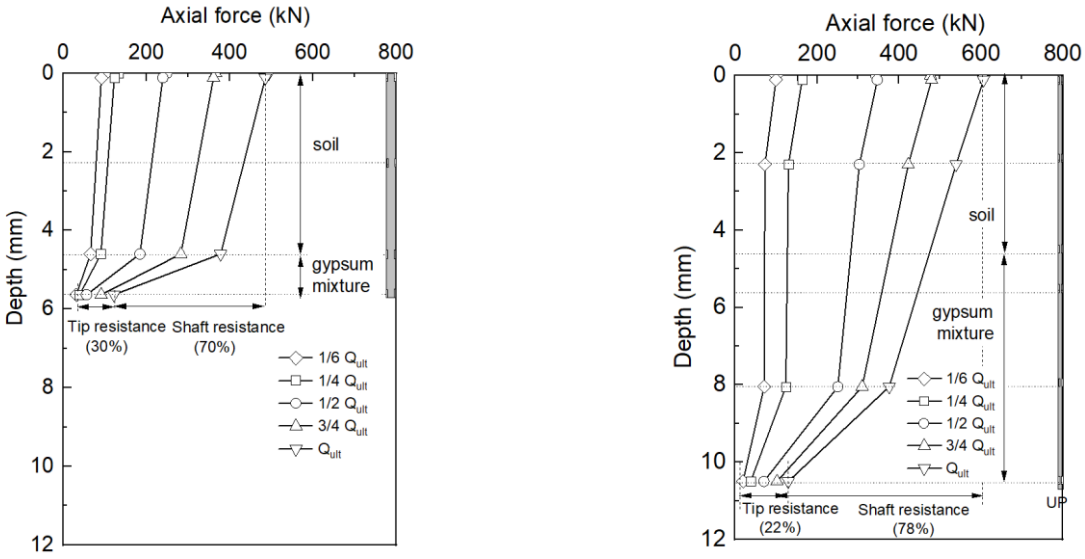

(a) EP3 (b) UP

Fig. 9 Axial force of EP3 and UP in the group pile without preloading ($Q_{ult:}$ 2200 kN, is the ultimate bearing capacity of the underpinned foundation without preloading)

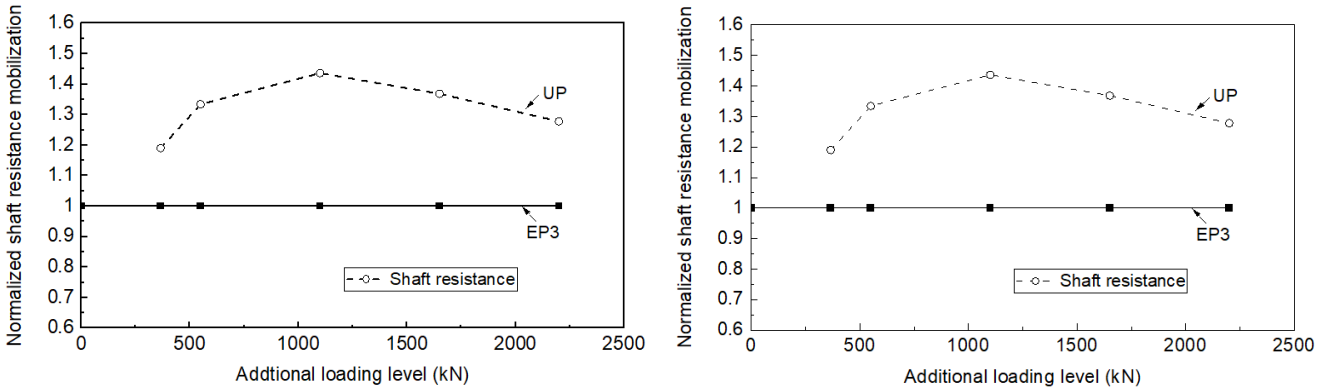

(a) Normalized shaft resistance of UP to EP3 (b) Normalized tip resistance of UP to EP3

Fig. 10 Normalized tip and shaft resistance of UP to EP3 under additional loading level to the plate

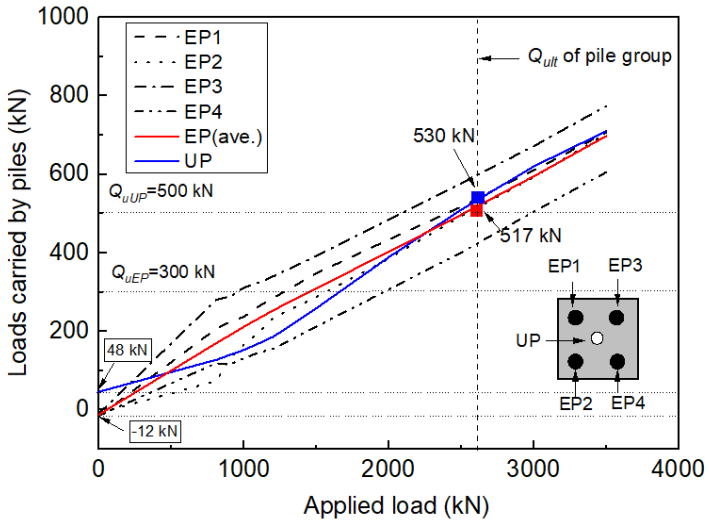

Fig. 11 Load-sharing behavior of the EPs and UP under additional loading on the raft after preloading ($Q_{ult:}$ 2600 kN, is the ultimate bearing capacity of the underpinned foundation with preloading obtained in Fig. 7)

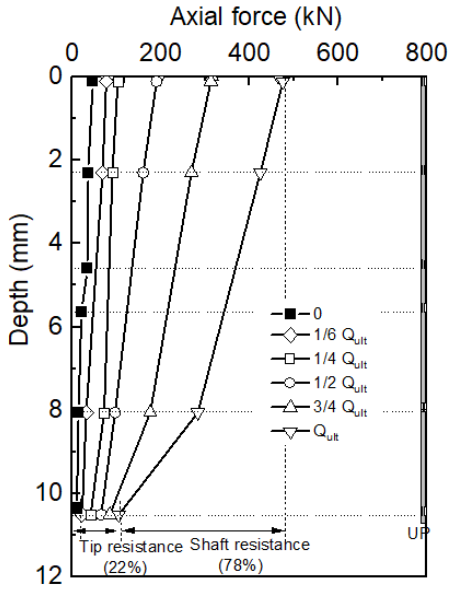

Fig. 12 Axial force distribution of UP under additional loading level for the case of with preloading (loading level is consistent with Fig. 9)

behaviors in both cases. This indicates that preloading has no influence on the stability of the foundation during the loading of the group pile. In accordance with the single-pile loading test, the bearing capacity of the group pile was estimated using the P-S criterion as 2200 and 2600 kN for group pile without and with preloading, respectively.

The purpose of underpinning an existing foundation is to share the loads caused by vertical extension to ensure the stability of the foundation. Therefore, understanding the load-sharing capacity of each pile is a key factor for an effective underpinning design. Fig. 8 presents the variation in the loads on each EP and the UP in the foundation without preloading. With increasing of the applied loads to the plate, both EPs and UP carry loads and the load-carrying capacity of the UP is higher than that of the EPs. When UP reaches the bearing capacity (500 kN, obtained from loading tests in Fig. 10), the increasing rate of load-carrying decreases. When the applied load is equal to the bearing capacity of the group pile, the load on the UP (600 kN) is 50% more than that on the EPs (average value: 400 kN) owing to the 60% higher stiffness of the UP, as shown in Fig. 10(a) (Kim *et al.* 2019, Wang *et al.* 2019).

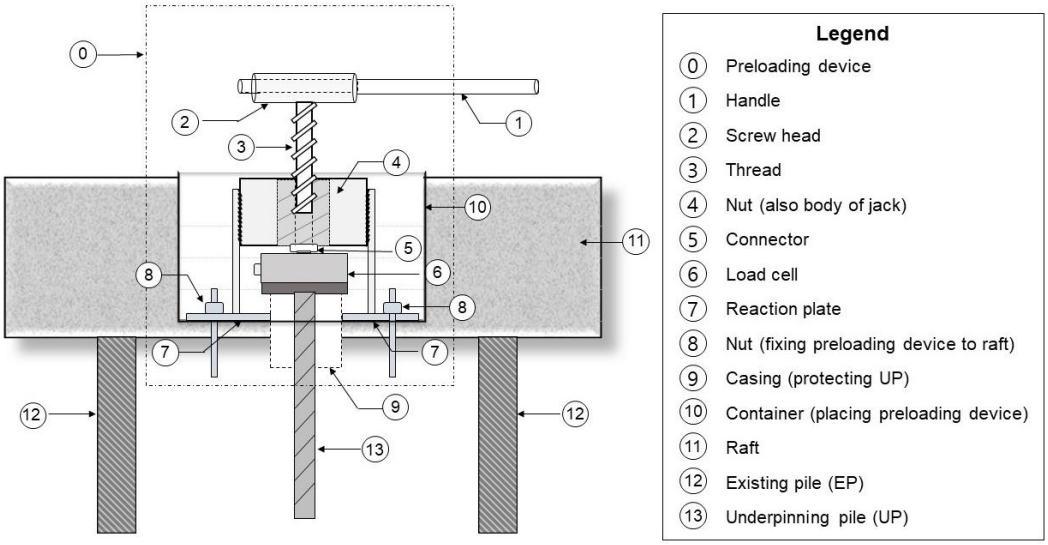

(a) Concept of screw-type preloading device

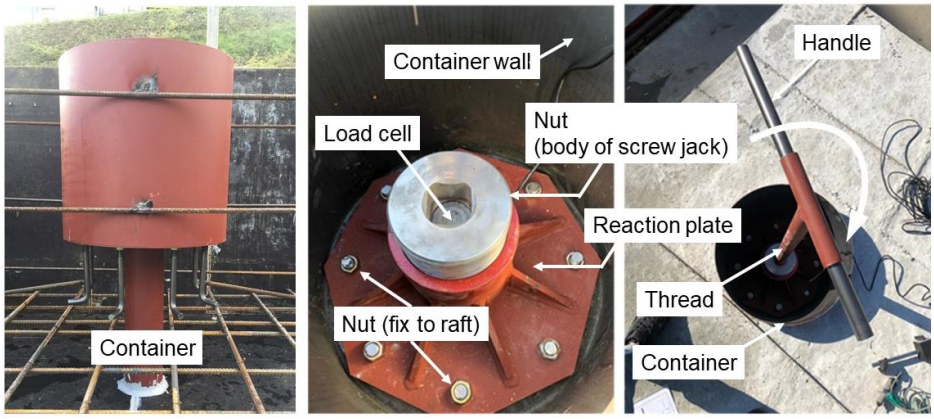

(b) Details of components

Fig. 13 Full-scale preloading device (screw type)

Fig. 9 shows the axial force distribution in EP3 and UP under additional loading to the plate. The shaft resistance and tip resistance in each pile were obtained based on the strain measurements. Under each loading level, the load carried by the head of UP is approximately 20-35% higher than that of EP3. The resistance of EP3 is mainly mobilized from the shaft along the pile in the gypsum mixture layer and the tip. The portion of the tip resistance of EP3 is 30% at the ultimate bearing capacity loading level, which is 8% more than that of UP, owing to the larger diameter of EP3. In contrast, because of the greater slenderness ratio of UP, the shaft resistance mainly mobilizes for resisting against applied loads, which is approximately 80%.

Fig. 10 depicts the normalized tip and shaft resistance of UP to EP3. At the initial additional loading level (less than 550 kN), because of the higher slenderness ratio of UP, the tip resistance mobilization of UP is less than that of EP. With increasing applied loads, both normalized tip and shaft resistance increase and become converged. The shaft resistance of UP is 20-40% higher than that of EP, whereas, the tip resistance is almost the same as EP. As seen in Fig. 8 or Fig. 9, the load carried by UP is 20-35 % larger than that of EP3. It indicates that the shaft resistance along the UP improves the load-sharing capacity. The load-carrying capacity is affected by its stiffness (i.e., the pile property and pile–soil interaction). The results imply that the shaft resistance makes a more significant contribution to increasing the pile stiffness than tip resistance.

Fig. 11 shows the load-sharing behavior of preloaded UP and EPs under additional loading. As a result of the prior load transfer between the EPs and UP owing to preloading, the initial load on the UP is positive at 48 kN, whereas the load on the EPs is negative. Under the loading level of the group pile bearing capacity, the load-sharing of the preloaded micropile is 530 kN, which is similar to the average value of the EPs, and 13% less than that of non-preloaded UP (600 kN). For better understanding of the load-sharing capacity of the preloaded UP, Fig. 18 displays the axial force on the UP with preloading under the same specific loading level for the case of without preloading, as shown in Fig. 11(b). The load on the pile increases with applied load and decreases with the depth. Fig. 12 shows that the preloading of the UP improves the mobilization of shaft resistances before the pile is subjected to additional loading. However, the comparison between Figs. 11(b) and Fig. 18 shows that under the same loading level on the pile group, the non-preloaded micropile carries more load than that of the preloaded UP. This is due to the mobilization of

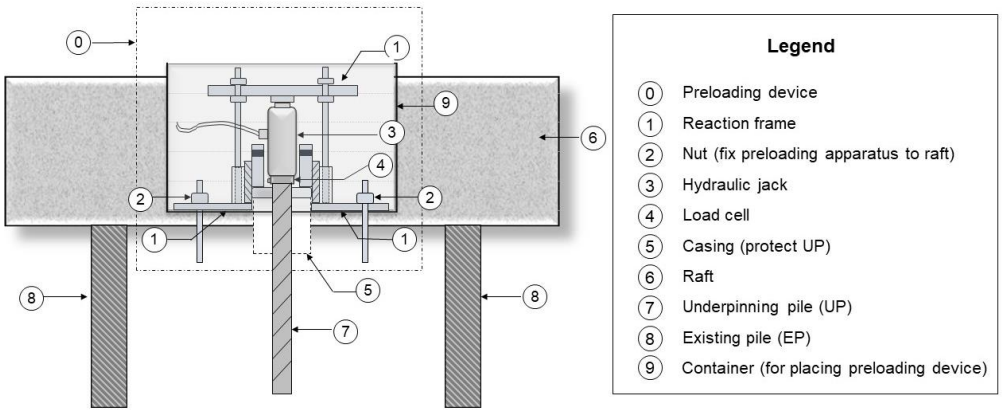

(a) Concept of hydraulic preloading device

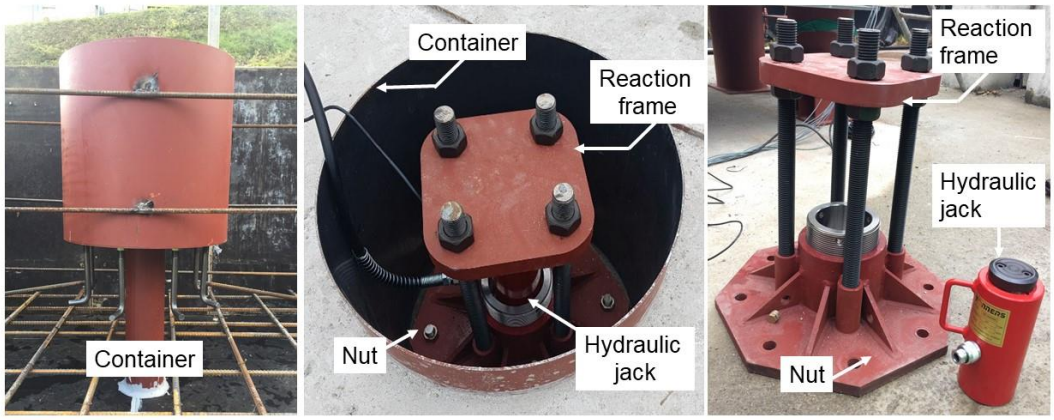

(b) Details of the components

Fig. 14 Full-scale preloading device (hydraulic-jack type)

shaft and tip resistance in the preloaded UP prior to additional loading, thereby leading to a reduction of the load-carrying capacity. Although non-preloaded UP carries more load than the preloaded micropile, at the loading level of ultimate bearing capacity of the group pile, the portion of tip and shaft resistance in non-preloaded UP is the same as that in the preloaded micropile. It implies preloading has no influence on the distribution of the tip and shaft resistance in a pile.

5. Full-scale structural test for preloading devices

Based on the working principle of the preloading method, two types of preloading devices were developed—a screw-jack type device and a hydraulic-jack type device. The devices were capable of applying preloading force at a practical construction site, and full-scale preloading tests for these preloading devices were carried out on a foundation with six model existing structures (ESs) and two model underpinning structures (USs) to verify the feasibility and load transfer performance of the preloading devices. ESs and USs represented EPs and UPs, respectively.

5.1 Design of preloading devices

5.1.1 Screw-jack type preloading device

Fig. 13 shows details of the screw-type preloading device, which consists of a screw jack and a reaction frame. The screw jack contains a screw, threaded hole, and loading handle. The screw jack is connected to the head of the UP, and the reaction frame is fixed to the raft of the existing foundation by eight nuts. The number of nuts is determined by considering the reaction force acting on the frame and the material strength of the frame. When the handle is turned clockwise, the device pushes the UP into the soil. This is accompanied by the application of reaction uplift force on the existing foundation. The advantage of this type of device over other types is that it is self-locking. This implies that when the rotational force on the screw is removed, the preloading device remains motionless and does not rotate backward, thereby improving safety and preventing load loss during load transfer.

5.1.2 Hydraulic-jack type preloading device

Fig. 14 presents the details of the hydraulic preloading device. The mechanism of this device is similar to that of the screw-type device; however, its operability is considerably superior to that of the screw jack. The hydraulic preloading device consists of a hydraulic jack and a reaction frame. Oil pressure is built by forcing oil into a cylinder. This pushes the UP into the soil and lifts the existing foundation upward through the reaction frame. It

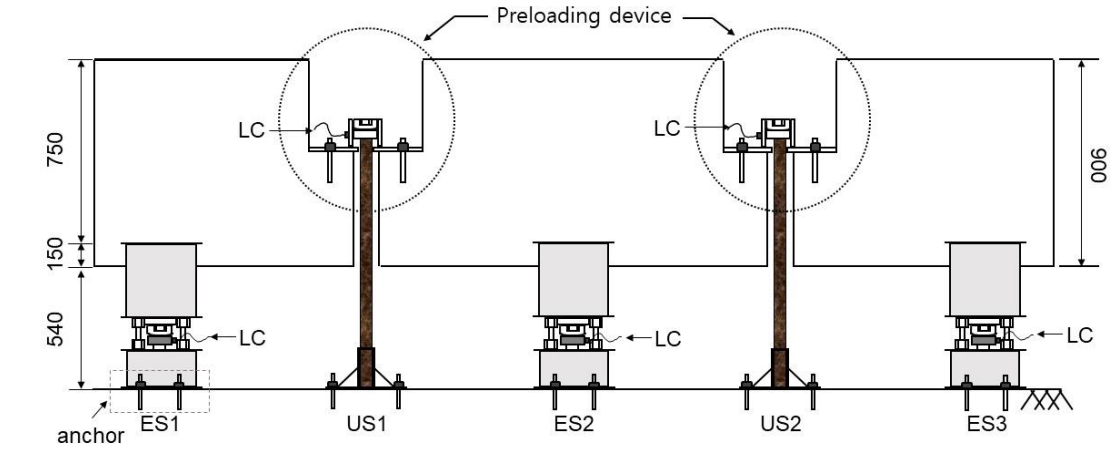

(a) Configuration of foundation (front view)

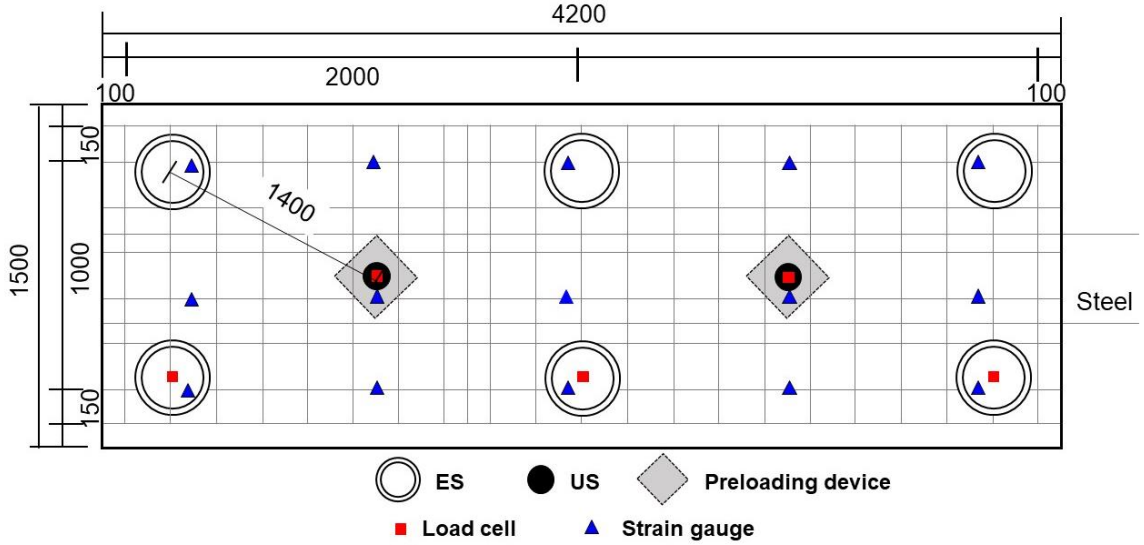

(b) Configuration of foundation (top view)

Fig. 15 Layout of full-scale foundation model (not to scale, unit: mm)

should be noted that in this full-scale test, the test model piles were installed as a fixed-bottom foundation for focusing on the operating mechanism of the preloading device without considering pile-soil interactions.

5.2 Configuration of foundation and installation

Fig. 15 illustrates the layout of the piled foundation for the full-scale test. The foundation includes a raft, six ESs, and two USs. Steel pipes with an outer diameter of 318 mm and a thickness of 10 mm were simulated as ES steel bars with a diameter of 50 mm. The reinforcing elements of conventional micropiles were used as USs. Two sets of preloading devices were placed on the USs. The raft was fabricated from cast-in-place concrete with reinforcing steel with a length of 4200 mm and a width of 1500 mm. Concrete strength was obtained as 30 MPa after 30 days of curing by performing an axial compressive strength test. In this full-scale test, all components were installed as a fixed-bottom foundation to focus on the operating mechanism of the preloading devices without considering pile-soil interactions.

Fig. 16 presents the instrumentation and installation in detail. Three load cells are installed on the front ESs (ES1, ES2, and ES3) and two on the USs (US1 and US2) to measure the load transfer during preloading. Strain gauges are attached to the reinforcing steel in the raft to measure its internal deformation.

5.3 Variation in loads on ESs and USs

The preloading process was as follows. First, a load of 40 kN was applied to US1 with an increment of 10 kN; then, a preload of 40 kN was applied to US2 in a similar manner. The load was maintained with the self-locking system of the screw jack in the screw-type device, whereas manual locking was required to maintain the hydraulic pressure in the hydraulic preloading device.

Fig. 17 shows the plots of the loads carried by all piles during the above preloading process for the two types of preloading devices. The load on ESs decreases as the preload on US1 increases and reaches 40 kN. Then, the

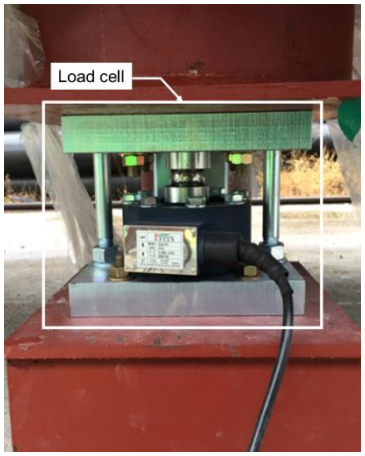

(a) Load cell on the ES

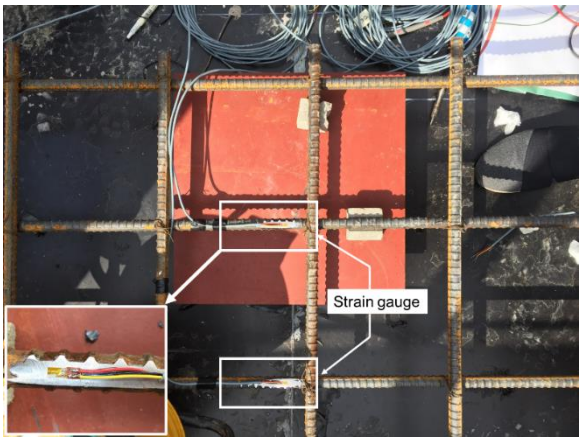

(b) Attachment of strain gauges

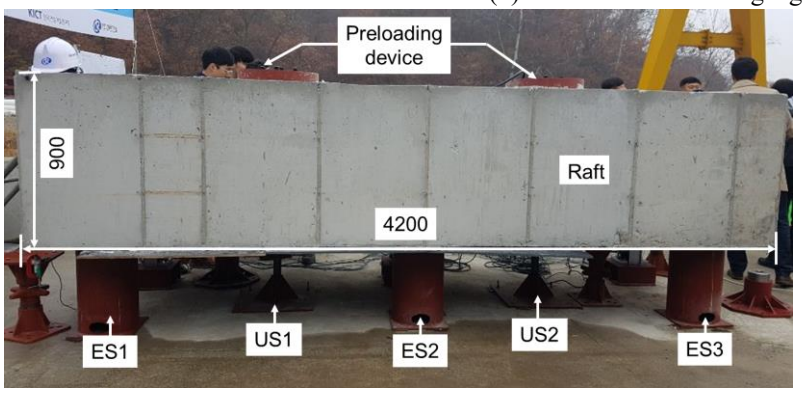

(c) Completion of the raft (after 30 days of concrete curing)

Fig. 16 Instrumentation and construction of full-scale foundation structure model (unit: mm)

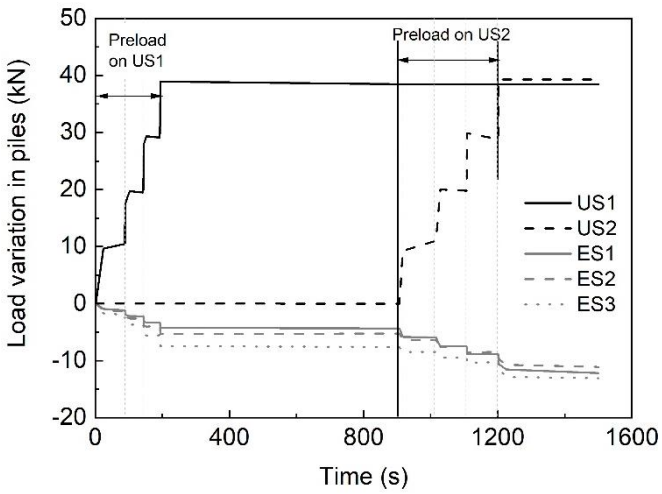

(a) Screw-jack device

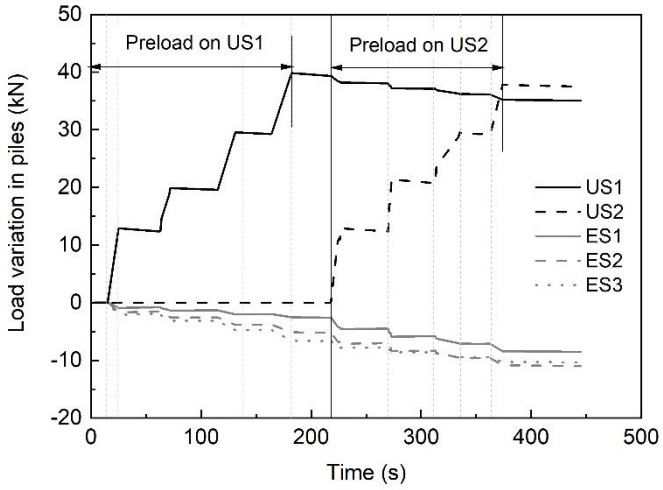

(b) Hydraulic-jack device

Fig. 17 Loads on ESs and USs vs. time under preload

loads on all piles remain constant until the preloading of US2 begins. The loads on the ESs decrease further as the preload on US2 increases and reaches 40 kN. The results clearly demonstrated load transfer from the ESs to the USs during preloading. The strain gauges measured only the minor deformation of the raft. The small variation in the strain measured during preloading showed that the reinforced concrete raft is rigid and does not deform significantly during preloading up to 80 kN.

To understand better the load transfer efficiency of the two types of preloading devices, Fig. 18 shows the plots of the load transfer between the ESs and USs measured by the load cells with respect to the preload on the USs. As three load cells were installed only on the front side for measuring the variation in the load on the ESs, the total reduction in the load on six ESs was assumed to be twice

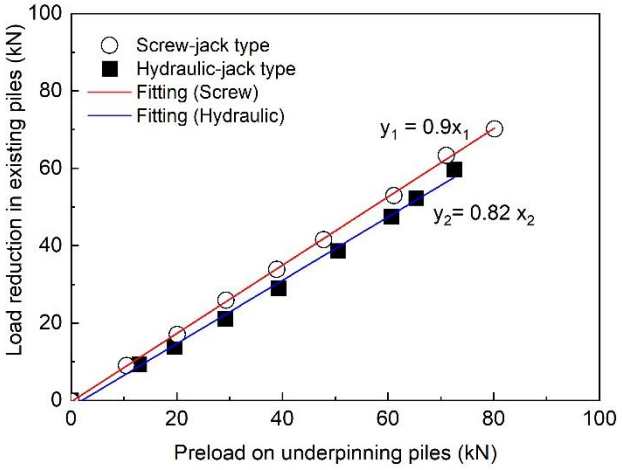

Fig. 18 Load loss during load transfer

the value measured by the three load cells. Fig. 18 shows that the total reduction in the load on the ESs increases linearly with the preload on the USs. The load transfer efficiency, which is defined as the slope of the curve, is 90% and 82% for the screw-type and hydraulic devices, respectively. As reported in previous studies, frictional loss is not preventable during jacking (Khazaei *et al.* 2016, Hong 2017). The load loss caused by frictional loss in the screw-type preloading device was reasonably assumed to be 10%. The manual locking system of the hydraulic device resulted in a low load maintenance capacity, as shown in Fig. 17(b). Therefore, the load transfer efficiency of the hydraulic device was lower than that of the screw-type device.

6. Conclusions

In this study, preloading devices were developed to transfer the loads from EPs to UPs in underpinned foundations to prevent the loads on existing foundations from exceeding their bearing capacity during vertical extension. The preloading devices applied preload on the UPs, thereby lifting existing foundations by the reaction force from the UPs. One model-scale reloading device and two types of full-scale preloading devices were developed. The model-scale device was developed for evaluating the load transfer mechanism of the preloading device in soil and the stability and load sharing among piles in a group pile under additional loading through centrifuge experiments. The full-scale devices were developed for practical application in the vertical extension work of existing buildings, and their feasibility and load transfer effect were verified by conducting full-scale structural experiments. The mechanisms of the devices and the experimental results are summarized as follows:

• A preloading device that used a pneumatic jack was developed for the centrifuge tests. In the preloading test, the load transfer effect of the preloading method was confirmed without loss during preloading. In the subsequent additional loading test, the load–settlement behavior and load-sharing behaviors of the group pile were evaluated. An appropriate preload on a UP (10% of its ultimate capacity in this study) had negligible influence on the stability of the underpinned foundation.

• The load-sharing capacity of a pile under additional loads was strongly affected by its stiffness. The LSR of a UP without preloading was 50% higher than that of an EP at the ultimate loading level owing to the 60% higher stiffness of the UP. The shaft resistance contributes to increasing the pile stiffness compared to the tip resistance. Preloading of the UP mobilizes tip and shaft resistance prior to additional loading, which reduces the stiffness of the UP and thus reduces the load-sharing capacity under additional loading. Therefore, in the practical design of existing underpinned foundations, it is recommended that a preloading method be applied where the allowable bearing capacity of EPs would be exceeded and a reduction in the load-sharing capacity of UPs should be considered.

• The full-scale preloading devices employed a screw system and a hydraulic jacking system to achieve load transfer from EPs to UPs. The advantage of the screw jack was its self-locking system, which remained motionless and did not rotate backward when rotational force was removed. The hydraulic-jack device provided better operability and higher injection capacity compared to the screw-type device. The constructability, operability, and load transfer effect of the screw-type and hydraulic preloading devices were successfully verified through full-scale structural experiments. The results demonstrated effective load transfer from the EPs to the UPs through the preload applied by turning the screw or injecting oil. The screw-type device provided a better load transfer efficiency of more than 90%, and 10% mechanical friction loss occurred in the device, whereas the load transfer efficiency of the hydraulic-jack type was 82 %.

Acknowledgments

This research was funded by a grant (21RERP-B099826-07) from the Residential Environment Research Program (RERP), which is funded by the Ministry of Land, Infrastructure and Transport of the Korean government

References

Alawneh, A.S., Malkawi, A.I. and Al-Deeky, H. (1999), "Tension tests on smooth and rough model piles in dry sand", *Can. Geotech. J.*, **36**(4),746-753. https://doi.org/10.1139/t98-104.

British Standards (2004), Eurocode 7: Geotechnical Design-Part 1: General Rules, British Standards, U.K.

Bruce, D.A. (1988), "Aspects of minipiling practice in the United States", *Ground Eng.*, **21**(8), 20-33.

Butcher, A.P., Powell, J.J. and Skinner, H.D. (2006), *Reuse of Foundations for Urban Sites: A Best Practice Handbook*, BRE Press, Watford, U.K.

Cho, H.I., Kim, H.S., Sun, C.G. and Kim, D.S. (2020), "Settlement prediction for footings based on stress history from Vs measurements", *Geomech. Eng.*, **20**(5), 371-384. https://doi.org/10.12989/gae.2020.20.5.371.

Dykeman, P. and Valsangkar, A.J. (1996), "Model studies of socketed caissons in soft rock", *Can. Geotech. J.*, **33**(5), 747-759. https://doi.org/10.1139/t96-100-321.

El Kamash, W. and Han, J. (2017), "Numerical analysis of existing foundations underpinned by micropiles", *Int. J. Geomech.*, **17**(6), 04016126. https://doi.org/10.1061/(ASCE)GM.1943-5622.0000833.

El Naggar, M.H. and Sakr, M. (2000), "Evaluation of axial performance of tapered piles from centrifuge tests", *Can. Geotech. J.*, **37**(6), 1295-1308. https://doi.org/10.1139/t00-049.

Essler, R. and Yoshida, H. (2004), *Jet Grouting*, *Ground Improvement*, 2nd Edition, Taylor & Francis, New York, U.S.A., 160-196.

FHWA (2000), *Micropile Design and Construction Guidelines-Implementation Manual*, FHWA-SA-97-070, Federal Highway Administration, Washington, D.C., U.S.A.

Hong, S. (2017), "Effect of prestress levels and jacking methods on friction losses in curved prestressed tendons", *Appl. Sci.*, **7**(8), 824. https://doi.org/10.3390/app7080824.

Horikoshi K. and Randolph, M.F. (1998), "A contribution to optimum design of piled rafts", *Geotechnique*, **48**(3), 301-317. https://doi.org/10.1680/geot.1998.48.3.301.

Horikoshi, K. and Randolph, M.F. (1996), "Centrifuge modelling of piled raft foundations on clay", *Geotechnique*, **46**(4), 741-752. https://doi.org/10.1680/geot.1996.46.4.741.

Horikoshi, K., Matsumoto T., Hashizume, Y., Watanabe, T. and Fukuyama, H. (2003), "Performance of piled raft foundations subjected to static horizontal loads", *Int. J. Phys. Modell. Geotech.*, **3**(2), 37-50. https://doi.org/10.1680/ijpmg.2003.030204.

Jang, Y.E. and Han, J.T. (2018), "Analysis of the shape effect on the axial performance of a waveform micropile by centrifuge model tests", *Acta Geotechnica*, **14**(2), 505-518. https://doi.org/10.1007/s11440-018-0657-2.

Juran, I., Benslimane, A. and Hanna, S. (2001), "Engineering analysis of dynamic behavior of micropile systems", *Transport. Res*, *Rec. J. Transport. Res. Board*, **1772**(1), 91-106. https://doi.org/10.3141/1772-11.

Khazaei, S., Wu, W., Shimada, H. and Matsui, K. (2016), "Effect of lubrication strength on efficiency of slurry pipe jacking", *Proceedings of the GeoShanghai International Conference 2006*, Shanghai, China, June.

Kim, D.H., Kim, J.H. and Jeong, S.S. (2019), "Estimation of axial stiffness on existing and reinforcing piles in vertical extension remodeled buildings", *Eng. Struct.*, **199**, 109466. https://doi.org/10.1016/j.engstruct.2019.109466.

Kim, D.S., Kim, N.R., Choo, Y.W. and Cho, G.C. (2013), "A newly developed state-of-the-art geotechnical centrifuge in Korea", *KSCE J. Civ. Eng.*, **17**(1), 77-84. https://doi.org/10.1007/s12205-013-1350-5.

Laefer D.F. (2011), "Quantitative support for a qualitative foundation reuse assessment tool", *Proceedings of the Geo-Frontiers 2011: Advances in Getotechnical Engineering*, Dallas, Texas, U.S. A., March.

Leung, C.R. and Ko, H.Y. (1993), "Centrifuge model study of piles socketed in soft rock", *Soils Found.*, **33**(3), 80-91. https://doi.org/10.3208/sandf1972.33.3_80.

Lutenegger, A.J. and Gerald, A.M. (1994), "Uplift capacity of small-diameter drilled shafts from in situ tests", *J. Geotech. Eng.*, **120**(8), 1362-1380. https://doi.org/10.1061/(ASCE)0733-9410(1994)120:8(1362).

Mayerhof, G.G. (1976), "Bearing capacity and settlement of pile foundations", *J. Geotech. Geoenviron. Eng.*, **102**, 195-228.

MOLIT. (2013), Housing Act, Korea Ministry of Land, Infrastructure and Transport:2 (in Korean).

Park, D.S. (2018) "Analyses of centrifuge modelling for artificially sensitive clay slopes", *Geomech. Eng.*, **16**(5), 513-525. https://doi.org/10.12989/gae.2018.16.5.513.

Qian, Z.Z., Lu, X.L., Yang, W.Z. and Cui Q. (2014), "Behaviour of micropiles in collapsible loess under tension or compression load", *Geomech. Eng.*, **7**(5). 477-493. http://doi.org/10.12989/gae.2014.7.5.477.

Wang, C., Han J.T., Jang, Y.E., Ha, I.S. and Kim, S.J. (2018), "Study on the effectiveness of preloading method on reinforcement of the pile foundation by 3D FEM analysis", *J. Kor. Geotech. Soc.*, **34**(1), 47-57. https://doi.org/10.7843/kgs.2018.34.1.47.

Wang, C., Han, J.T. and Jang, Y.E. (2019), "Experimental investigation of micropile stiffness affecting the underpinning of an existing foundation", *Appl. Sci.*. **9**(12), 2495. https://doi.org/10.3390/app9122495.

Wang, C., Han, J.T. and Jang, Y.E. (2020), *Investigation of Effectiveness of Preloading Method for Existing Foundation Underpinning by Centrifuge Tests*, in *Geotechnics for Sustainable Infrastructure Development*. Springer, Singapore, 61-67.

Wang, C., Zhou, S., Wang, B., Guo P. and Su, H. (2016), "Settlement behavior and controlling effectiveness of two types of rigid pile structure embankments in high-speed railways", *Geomech. Eng.*, **11**(6), 847-865. https://doi.org/10.12989/gae.2016.11.6.847.

Wood, D.M. (2004), *Geotechnical Modelling*, 1st Edition, CRC Press, Boca Raton, Florida, U.S.A.

IC